Supporting Information

Double-helix Supramolecular Nanofibers Assembled from Negatively Curved Nanographenes

Kenta Kato,[1,†,§] Kiyofumi Takaba,[2,†] Saori Maki-Yonekura,[2,†] Nobuhiko Mitoma,[1,3,4] Yusuke Nakanishi,[5] Taishi Nishihara,[1,3,6] Taito Hatakeyama,[7] Takuma Kawada,[7] Yuh Hijikata,[1,8,9] Jenny Pirillo,[8,9] Lawrence T. Scott,[10] Koji Yonekura,[2,11,12,*] Yasutomo Segawa,[1,3,13,14,*] and Kenichiro Itami[1,3,8,*]

Correspondence to: yone@spring8.or.jp (K.Y.), segawa@ims.ac.jp (Y.S.), itami@chem.nagoya-u.ac.jp (K.I.)

† These authors contributed equally.

Materials and Methods

Synthesis, purification, and identification

Unless otherwise noted, all materials including dry solvent were obtained from commercial suppliers and used without further purification. All reactions were performed using standard vacuum-line and Schlenk techniques. Work-up and purification procedures were carried out with reagent-grade solvents under air. 1,3,5,7,9-Pentakis(pinacolatoboryl)corannulene (**4**) and tetrakis(pinacolatoboryl)corannulene **2** (regioisomeric mixture) were synthesized according to the reported procedure.[S1]

Analytical thin-layer chromatography (TLC) was performed using E. Merck silica gel 60 F254 precoated plates (0.25 mm). The developed chromatograms were analyzed by UV lamp (254 or 365 nm). Flash column chromatography was performed with E. Merck silica gel 60 (230–400 mesh). The high-resolution mass spectra (HRMS) were conducted on a Bruker Daltonics Ultraflex III TOF/TOF (MALDI-TOF MS). Melting points were measured on an MPA100 Optimelt automated melting point system. Nuclear magnetic resonance (NMR) spectra were recorded on a JEOL ECA 600II spectrometer with UltraCool probe (^{1}H 600 MHz, ^{13}C 150 MHz) spectrometer. Chemical shifts for ^{1}H NMR are expressed in parts per million (ppm) relative to C_2HDCl_4 (δ 5.98 ppm). Chemical shifts for ^{13}C NMR are expressed in ppm relative to $C_2D_2Cl_4$ (δ 73.79 ppm). Data are reported as follows: chemical shift, multiplicity (s = singlet, d = doublet, t = triplet, m = multiplet, br = broad), coupling constant (Hz), and integration.

Atomic force microscopy (AFM) measurement of the fibrous structures of **1-H**

AFM measurements were performed using a Dimension FastScan (Bruker) at room temperature and under atmospheric conditions with a silicon tip on silicon nitride cantilevers (FastScan-C, Bruker) in tapping mode. Organogels of **1-H** were formed on a SiO_2 substrate by slowly evaporating the CH_2Cl_2 solution of **1-H**.

Transmission electron microscopy (TEM) measurement of the fibrous structures of **1-H**

High-resolution TEM observation was performed on a JEOL JEM-2100F at an acceleration voltage of 80 kV under a pressure of 10^{-5} Pa. The gel of **1-H** in CH_2Cl_2 was broken by shaking, and 5 drops of the supernatant were deposited onto carbon-coated copper grids. Prior to the observation, the sample was dried under vacuum for 30 min at ambient temperature. TEM images were recorded on a Gatan MSC 794 1k × 1k CCD camera with a typical exposure time of 0.3 s.

Photophysical Measurements

UV-vis absorption spectrum of the diluted dichloromethane solution of **1-H** (ca. 10^{-6} M) in a 1 cm square quartz cell was recorded on a Shimadzu UV-3600 spectrometer with a resolution of 0.5 nm. Emission spectra of the diluted degassed dichloromethane solution of **1-H** (ca. 10^{-7} M) in a 1 cm square quartz cell was recorded on an F-4500 Hitachi spectrometer with a resolution of 0.4 nm and automatically corrected by instrumental function. Absolute fluorescence quantum yield of the diluted degassed dichloromethane solution of **1-H** (ca. 10^{-7} M) in a 1 cm square quartz cell was determined with a Hamamatsu C9920-02 calibrated integrating sphere system equipped with multichannel spectrometer (PMA-11). Emission spectra of the gel state of **1-H** were recorded using a monochromator attached to a thermoelectrically cooled charge-coupled device camera (Princeton Instruments, ProEM). The excitation light source was a wavelength-tunable optical parametric amplifier system based on a Yb:KGW (potassium gadolinium tungstate) regenerative amplified laser with a pulse duration of 200 fs and repetition rate of 200 kHz.

X-ray crystallography of **1-Cl**

Details of the crystal data and a summary of the intensity data collection parameters for **1-Cl** are listed below. A suitable crystal of **1-Cl** obtained from the 1,2-dichloroethane solution was mounted with mineral oil on a MiTeGen MicroMounts and transferred to the goniometer of the kappa goniometer of a RIGAKU XtaLAB Synergy-S system with 1.2 kW MicroMax-007HF microfocus rotating anode (Graphite-monochromated Mo Kα radiation (λ = 0.71073 Å)) and PILATUS200K hybrid photon-counting detector. Cell parameters were determined and refined, and raw frame data were integrated using CrysAlis^{Pro} (Agilent Technologies, 2010). The structures were solved by direct methods with (SHELXT)[S2] and refined by full-matrix least-squares techniques against F^2 (SHELXL-2018/3)[S3] by using Olex2 software package.[S4] The intensities were corrected for Lorentz and polarization effects. The non-hydrogen atoms were refined anisotropically. Hydrogen atoms were placed using AFIX instructions. The CIF data can be obtained free of charge from Crystallographic data and structure refinement details of **1-Cl** are summarized in Table S2. The Cambridge Crystallographic Data Centre via www.ccdc.cam.ac.uk/data_request/cif (CCDC 2039243).

Electron diffraction crystallography of **1-H**

1. Sample screening and data collection of rotational electron diffraction patterns

Sample solution (1,1,2,2-tetrachloroethane) containing the crystalline nanofiber bundles of **1-H** was dispersed with ethanol and applied onto a holey carbon-coated copper grid (Quantifoil R1.2/1.3, Quantifoil Micro Tools GmbH) with 200 mesh. Excess solution on the grid was blotted off with filter paper from the back side and dried at room temperature. Crystals on the grids were then screened at a cryogenic temperature of ~100 K with a JEM-2100 electron microscope (JEOL Ltd., Japan). Needle-shaped crystals obtained from one sample solution showed good diffraction patterns, and this was selected for 3D data collection.

The sample containing well-diffracting nanofiber bundles was prepared as above and examined with a CRYO ARM 300 microscope (JEOL Ltd., Japan) operated at an accelerating voltage of 300 kV and equipped with an in-column type energy filter. Diffraction patterns were recorded on a scintillator-based CMOS camera (XF416, TVIPS GmbH, Germany) at a specimen temperature of ~ 98 K. One crystal was parallel illuminated with a ~5 μm beam and no selected area aperture inserted at an electron dose rate of ~0.02 $e^-/Å^2 \cdot s$. Sequential diffraction frames were collected from one crystal by continuously rotating the sample stage from –68º to 68º at a goniometer rotation speed of 1°/s. Total 55 rotational series were collected in a semi-automated manner by combined use of SerialEM[S5] and ParallEM.[S6,7] A report on details of this data collection protocol was reported.[S8] All datasets were taken with an energy slit adjusted to select only electrons with energy loss less than 10 eV. The camera length was calibrated to be 1245 mm from gold sputtered on carbon film as a standard.

2. Data processing and structure determination

Diffraction stacks, each of which comprises 140 raw frames with 4k × 4k pixels, were first × 2 binned (2048 × 2048 pixels) for speeding up the following steps. Diffraction datasets were then subjected to automatic processing with KAMO,[S9] which carried out indexing, integration, scaling and merging by using XDS,[S10] Pointless,[S11] XSCALE,[S12] and BLEND.[S13] Total 46 datasets were merged and the high-resolution limit was determined to be 0.85 Å, where a $CC_{1/2}$ (the correlation coefficient between random half data sets) value was greater than 50%.[S14] The lattice group was

determined to be tetragonal with lattice parameters of $a = b = 34.61$ Å, $c = 16.51$ Å. Data collection statistics and crystal parameters are summarized in Table S3.

An initial structure was solved with a space group $P4_2$ by molecular replacement starting from the structure of a **1-Cl** using Phaser.[S15] An asymmetric unit contained four **1-H** molecules ($Z' = 4$). The same solution was obtained with this space group setting by the direct method using SHELXD.[S16] The structure was then refined with Phenix[S17] and SHELXL[S3] using anisotropic displacement parameters for all carbon atoms. Dependence on the experimental wavelength (λ) of an empirical extinction correction factor (EXTI)[S18] was not clear for electron diffraction. Here we excluded diffraction data in a lower resolution range ($d > 7$ Å) and used a λ value of 1.0 Å in the formula below,

$$F_c' = F_c\, k\, [1 + 0.001\, x\, F_c^2\, (1.0)^3 / \sin(2\theta)]^{-1/4} ,$$

where k is the overall scale factor and x is extinction factor to be refined. This provisional correction significantly reduced an error factor (R) between the model and the experimental data, and less affected the atomic positions. The positions of all hydrogen atoms were generated as a riding model with AFIX instructions. C–C bond distances were restrained based on the structure of **1-H**. Restraints in atomic displacement parameters (ADPs) were adjusted with RIGU, SIMU and ISOR instructions so that ADPs were within reasonable values. Probably due to disordering, solvent molecules (1,1,2,2-tetrachloroethane) could not be placed suitably to solvent accessible voids. The final R_1 value is 0.1647. The CIF data can be obtained free of charge from The Cambridge Crystallographic Data Centre via www.ccdc.cam.ac.uk/data_request/cif (CCDC 2039244).

DFT calculation

The Gaussian 16 program[S19] running on a NEC LX 110Rh system was used for optimization (B3LYP/6-31G(d)).[S20,S21] Structures were optimized without any symmetry assumptions.

Synthesis of **1-H**

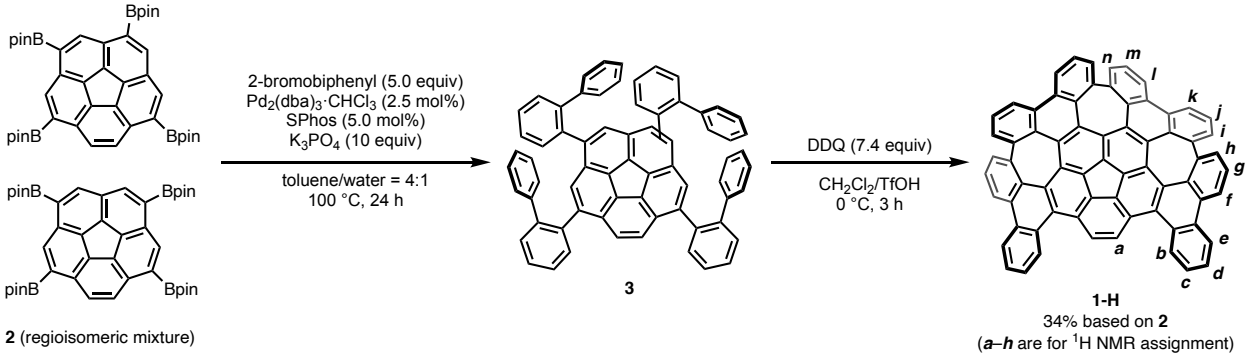

To a solution of $Pd_2(dba)_3 \cdot CHCl_3$ (34.3 mg, 33.1 μmol, 2.5 mol%) and SPhos (27.2 mg, 66.2 μmol, 5.0 mol%) in toluene (10 mL) were added $(Bpin)_4$corannulene **2** (1.00 g, 1.33 mmol, 1.0 equiv), 2-bromobiphenyl (1.55 g, 6.63 mmol, 5.0 equiv) and solution of K_3PO_4 (2.81 g, 13.2 mmol, 10 equiv, in 2.6 mL water), and the resultant mixture was stirred at 100 °C for 24 h under argon. After cooling the mixture to room temperature, the reaction mixture was extracted with chloroform. The combined organic layer was dried over $MgSO_4$, and the solvent was removed under reduced pressure. The crude material was purified by silica-gel column chromatography (eluent: hexane/chloroform = 10:0 to 6:4) to afford a mixture of 1,3,5,8- and 1,3,6,8-tetrakis(2-biphenylyl)corannulene (**3**, 788 mg), which was used in the next reaction without further purification.

A solution of mixture of **3** (374 mg) and 2,3-dichloro-5,6-dicyano-*p*-benzoquinone (DDQ; 730 mg, 3.20 mmol, 7.4 equiv) in dry dichloromethane (65 mL) was added dropwise to the mixture of dry dichloromethane (5.5 mL) and trifluoromethanesulfonic acid (TfOH; 2.2 mL) at 0 °C for 30 min. After stirring for an additional 2.5 hours, the reaction mixture was quenched by Et_3N (14 mL) and the solvent was removed under reduced pressure. The crude mixture was separated by silica-gel column chromatography (eluent: hexane/chloroform = 1:1) to afford **1-H** as a yellow powder (183 mg, 34% yield based on **2**). The ^{1}H NMR signals were assigned according to DFT calculation (Fig. S5).

Method for the formation of an organogel: The saturated solution of **1-H** (1.0 mL) was put on the bottom of a 3-mL screw-capped vial (vial A). Vial A was put into a 20-mL screw-capped vial (vial B). Hexane (ca. 5 mL) was poured into vial B and the cap of vial B was closed to fill the vials with hexane vapor. After 1 day, organogel was formed on the bottom of vial A. The supernatant was removed from the vial by tilting the vial slowly. After the weight of the organogel was recorded, the organogel was fully dried to recover **1-H**. CGC was determined as the weight ratio of [the recovered **1-H**]/[the organogel].

^{1}H NMR (600 MHz, $C_2D_2Cl_4$, 25 °C) δ 9.30 (d, J = 7.8 Hz, 1H, ***b***), 8.71 (s, 1H, ***a***), 8.67 (d, J = 7.2 Hz, 1H, ***e***,***f***,***k***,***l***), 8.60 (d, J = 7.2 Hz, 1H, ***e***,***f***,***k***,***l***), 8.57 (d, J = 8.4 Hz, 2H, ***e***,***f***,***k***,***l***), 7.81 (t, J = 6.0 Hz, 1H, ***c***,***d***,***g***,***j***,***m***), 7.79 (t, J = 6.6 Hz, 1H, ***c***,***d***,***g***,***j***,***m***), 7.72 (t, J = 7.2 Hz, 1H, ***c***,***d***,***g***,***j***,***m***), 7.71 (t, J = 7.2 Hz, 1H, ***c***,***d***,***g***,***j***,***m***), 7.67 (t, J = 7.8 Hz, 1H, ***c***,***d***,***g***,***j***,***m***), 7.46 (d, J = 7.8 Hz, 1H, ***h***,***i***,***n***), 7.42 (d, J = 7.8 Hz, 1H, ***h***,***i***,***n***), 7.21 (d, J = 6.6 Hz, 1H, ***h***,***i***,***n***); ^{13}C NMR (150 MHz, $C_2D_2Cl_4$, 25 ºC) δ 139.44 (4°), 139.41 (4°), 138.82 (4°), 134.08 (4°), 134.05 (4°), 133.08 (4°), 133.26 (4°), 132.61 (4°), 132.55 (4°), 132.08 (CH), 131.75 (4°), 131.02 (4°), 130.91 (4°), 130.83 (4°), 130.80 (4°), 130.75 (CH), 130.61 (CH), 130.43 (4°), 130.01 (4°), 129.43 (4°), 129.08 (4°), 129.00 (CH), 128.60 (CH), 128.01 (CH, 2C), 127.61 (CH), 127.50 (CH), 127.43 (4°), 127.27 (4°), 126.87 (4°),

126.70 (CH), 123.29 (CH), 121.44 (CH), 121.39 (CH, 2C), one carbon (4°) could not be assigned; HRMS (MALDI-TOF MS) *m/z* calcd for $C_{68}H_{28}$ $[M\cdot]^+$: 844.2191, found: 844.2191; mp: >300 ºC.

Synthesis of **1-Cl**

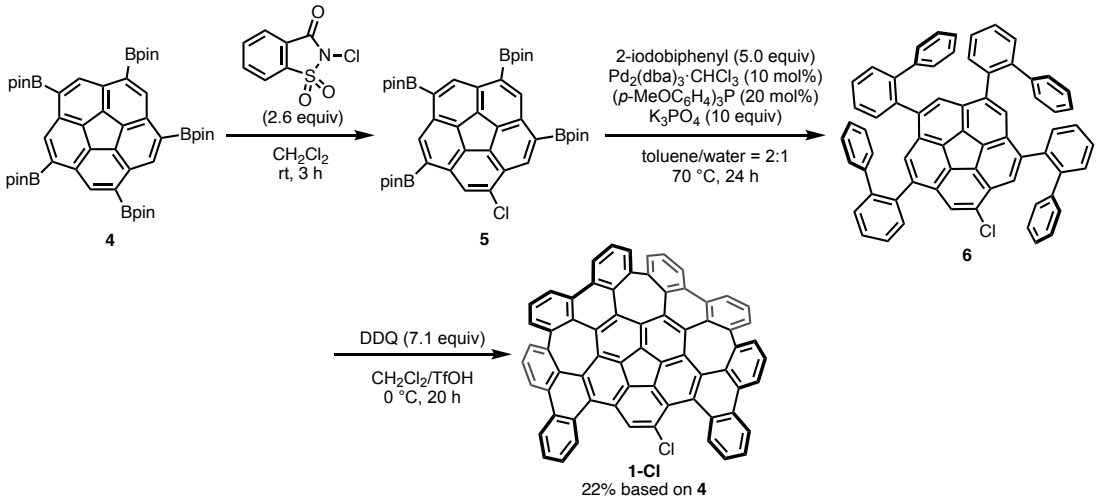

A solution of **4** (1.10 g, 1.25 mmol, 1.0 equiv) and *N*-chlorosaccharin[S22] (712 mg, 3.27 mmol, 2.6 equiv) in dichloromethane (12.5 mL) was stirred at rt for 1 h. Hexane (60 mL) was added to the reaction mixture to precipitate saccharin derivatives. The suspension was filtered over a pad of Celite® and the solution was evaporated under reduced pressure. Additional hexane (75 mL) was added and filtered over a pad of Celite®. The filtrate was concentrated under reduced pressure. The compound **5** was obtained as a yellow foam (1.01 g), which was used for the next reaction without further purification.

To a solution of $Pd_2(dba)_3{\cdot}CHCl_3$ (7.3 mg, 8.0 μmol, 10 mol%) and tris(4-methoxyphenyl)phosphine (5.6 mg, 16 μmol, 20 mol%) in toluene (1.33 mL) were added **5** (63.0 mg, 80.0 μmol, 1.0 equiv), 2-iodobiphenyl (112 mg, 400 μmol, 5.0 equiv) and a solution of K_3PO_4 (170 mg, 800 μmol, 10 equiv) in water (0.67 mL). The reaction mixture was stirred at 70 °C for 24 h under argon. After quenching the reaction with water (5.0 mL), the reaction mixture was extracted with dichloromethane. The combined organic layers were dried over Na_2SO_4, and the filtrate was concentrated under reduced pressure. The residue was washed by MeOH and hexane to afford **6** (44.9 mg), which was used for the next reaction without further purification.

A solution of mixture of **6** (44.9 mg) and DDQ (81.0 mg, 360 μmol, 7.1 equiv) in dry dichloromethane (8.5 mL) was added dropwise to mixture of dry dichloromethane (1.0 mL) and TfOH (0.5 mL) at 0 °C for 30 min. After stirring for additional 20 hours, the reaction mixture was quenched by Et_3N (1.0 mL) and the volatile was removed under reduced pressure. Methanol (20 mL) was added and the resultant suspension was filtered. The residue was purified by silica-gel column chromatography (eluent: chloroform) to afford **1-Cl** as a yellow powder (22.0 mg, 22% yield based on **4**).

^{1}H NMR (600 MHz, $C_2D_2Cl_4$, 25 ºC) δ 9.07 (d, *J* = 7.8 Hz, 1H), 8.76 (d, *J* = 7.2 Hz, 1H), 8.63-8.61 (m, 4H), 8.55 (d, *J* = 7.8 Hz, 1H), 8.49 (d, *J* = 8.4 Hz, 1H), 8.46 (br s, 1H), 8.40-8.38 (m, 2H), 8.29 (s, 1H), 7.92 (t, *J* = 7.2 Hz, 2H), 7.88-7.82 (m, 3H), 7.72-7.67 (m, 2H), 7.52 (t, *J* = 7.8 Hz, 2H), 7.42 (d, *J* = 8.4 Hz, 1H), 7.38 (d, *J* = 7.2 Hz, 1H), 7.27 (br s, 1H), 7.18 (d, *J* = 7.8 Hz, 1H), 7.04 (br s, 1H), 6.98 (d, *J* = 6.6 Hz, 1H); ^{13}C NMR (150 MHz, $C_2D_2Cl_4$, 25 °C) δ 140.02 (4°), 139.53 (4°), 139.32 (4°), 138.99 (4°), 138.76 (4°), 137.99 (4°), 137.87 (4°), 136.19 (4°), 135.86 (4°), 134.149 (4°), 133.86 (4°), 133.10 (CH), 132.59 (4°), 132.55 (4°), 132.22 (4°), 132.12 (4°), 132.07 (4°), 131.75 (CH), 131.71 (CH), 131.68 (4°), 131.54 (CH), 131.39 (4°), 131.33 (4°), 131.23 (CH), 131.00 (4°), 130.86 (4°), 130.77 (4°), 130.65 (4°), 130.49 (4°), 130.40 (4°),130.19 (4°),

130.13 (CH), 129.96. (4°), 129.53 (CH), 129.51 (4°), 129.29 (4°), 129.13 (4°), 128.86. (CH), 128.67. (4°), 128.63 (4°), 128.60 (4°), 128.56 (4°), 128.40 (CH), 128.35 (CH), 128.16 (4°), 127.86 (CH), 127.73. (CH), 127.56 (4°), 127.17 (CH), 126.97 (4°), 126.80 (4°), 126.76 (CH), 126.43 (4°), 125.32 (CH), 123.59 (CH), 122.70 (CH), 122.37 (CH), 121.74 (CH), 121.53 (CH), 121.41 (CH), 120.54 (CH), 120.19 (4°), four carbon atoms (4°×2, CH×2) could not be assigned; HRMS (MALDI-TOF MS) *m/z* calcd for $C_{68}H_{27}Cl$ $[M\cdot]^+$: 878.1801, found: 878.1776; mp: >300 ºC.

Table S1. Crystallographic Data and Structure Refinement Details of **1-Cl**.

	1-Cl·2.5$C_2H_4Cl_2$
formula	$C_{141}H_{64}Cl_7$
fw	2006.07
T (K)	123(2)
λ (Å)	0.71073
cryst syst	Triclinic
space group	P-1
a (Å)	14.0110(7)
b (Å)	14.8283(6)
c (Å)	25.9612(9)
α (deg)	79.517(3)
β (deg)	82.011(4)
γ (deg)	61.809(5)
V (Å^3)	4665.8(4)
Z	2
D_{calc} (g·cm^{-3})	1.428
μ (mm^{-1})	0.275
F(000)	2058
cryst size (mm)	0.03 × 0.03 × 0.02
2θ range (deg)	4.736–49.998
reflns collected	54449
indep reflns/R_{int}	16225/0.1500
params	1379
GOF on F^2	1.047
R_1, wR_2 [$I>2\sigma(I)$]	0.1185, 0.2889
R_1, wR_2 (all data)	0.2539, 0.3644

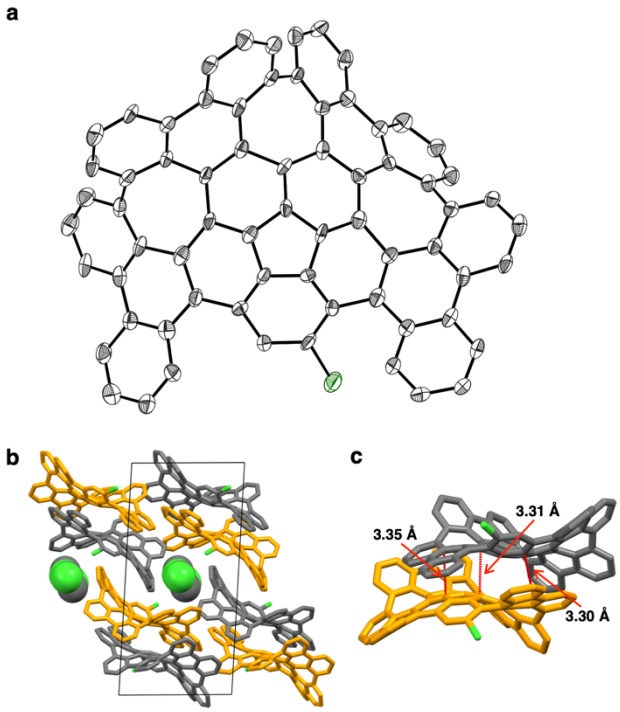

Fig. S1. (**a**) ORTEP drawing of **1-Cl** with 50% probability determined by X-ray crystallography. One of two crystallographically inequivalent parts, hydrogen atoms, and solvent molecules (1,2-dichloroethane) are omitted for clarity. (**b**) Packing structure of **1-Cl**. (**c**) The C–C short contacts (Å) seen in the π-π dimer of **1-Cl**. The positively curved corannulene center also contributes the efficient π-π interaction.

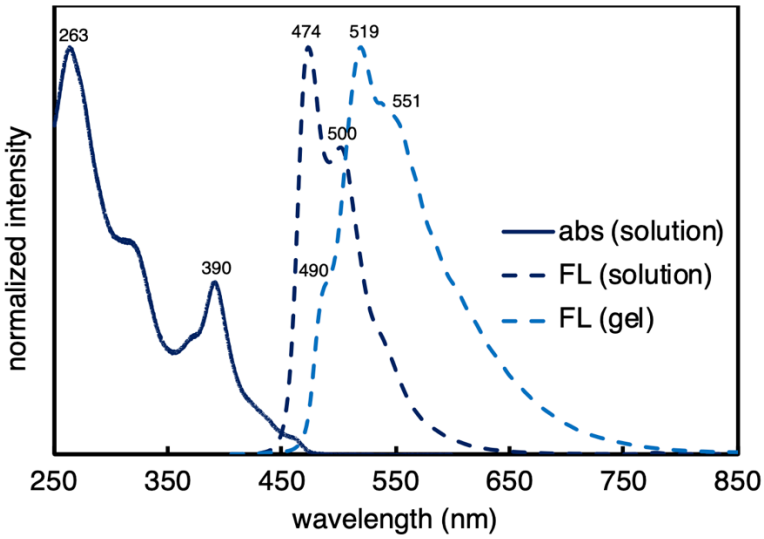

Fig. S2. A UV–Vis absorption spectrum (abs; solid line) and fluorescence spectra (FL; dotted lines) of **1-H** in dichloromethane and in the gel state. Fluorescence spectra were recorded upon excitation at 350 nm (solution) or 390 nm (gel). The wavelengths (nm) of the peak top values were indicated.

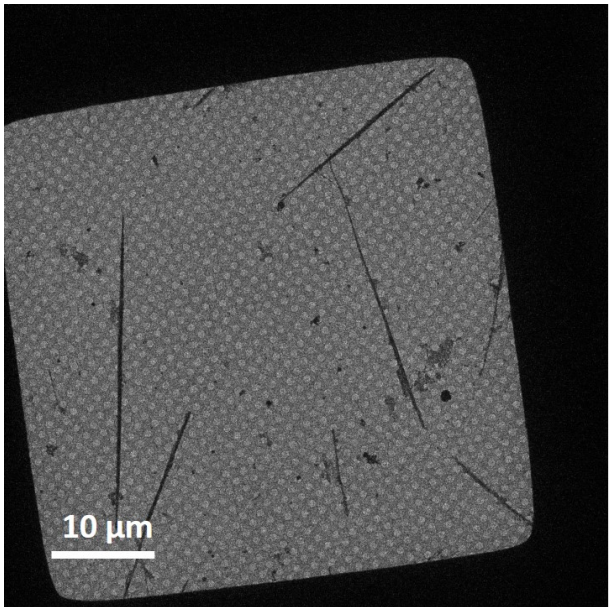

Fig. S3. A typical image of fibrous microcrystals distributed on the holey carbon film. Take at 400×. Diffraction patterns were collected from single fibrous microcrystal with a diameter of ≤ 1 µm.

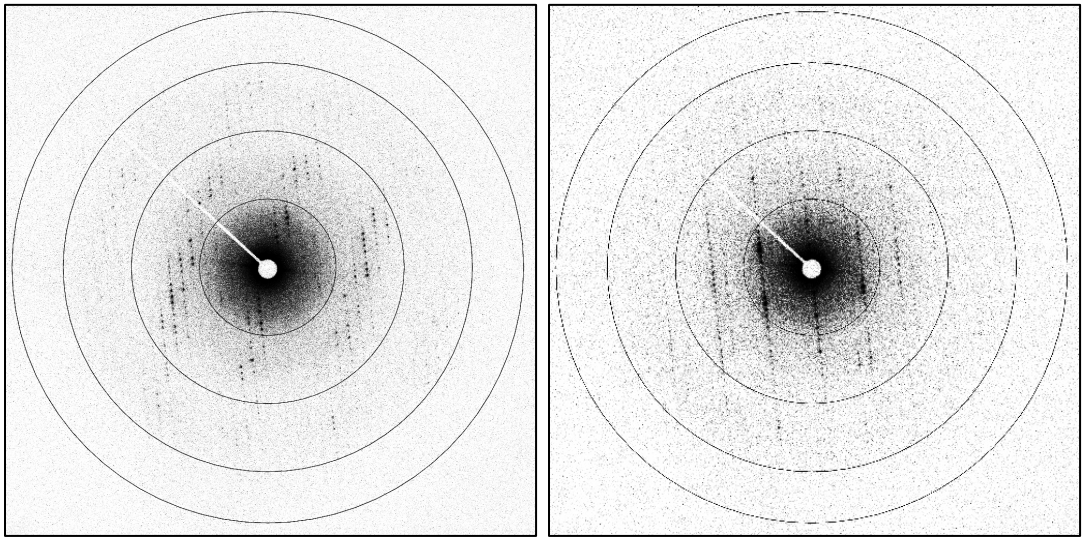

Fig. S4. Representative frames of energy-filtered electron diffraction (eEFD) patterns in a rotation angle of –4° ~ –3° (left) and +7° ~ +8° (right). Concentric circles indicate 3, 1.5, 1.0 and 0.8 Å resolution rings.

Table S2. Data and refinement statistics of the electron diffraction of **1-H.**

Experimental details	
λ (Å)	0.0197 (300 kV)
T (K)	98
Rotation speed (°/s)	1.00
Rotation range (°)	–68.00 to 68.00 (137)
Exposure time per frame (s)	1.00
Spot size	7
Illumination angle size (α)	5
Beam size (μm)	~ 5
Camera length (mm)	1245
No. of rotation datasets	46
Crystallographic data	
Crystal system	Tetragonal
Resolution (Å)	17.31 – 0.85 (0.87 – 0.85)
θ range (°)	0.081 – 0.66
h, k, l_{max}	40, 40, 19
No. of total reflections	3,226,335
No. of unique reflections	17,516
Completeness (%)	100.0 (100.0)
$\langle I/\sigma(I)\rangle$	15.56 (8.48)
$CC_{1/2}$ (%)	99.3 (58.0)
R_{sym} (%)	56.1 (81.9)
Refinement	
Chemical formula (refined)	$C_{272}H_{112}$
Formula weight	3379.61
Space group	$P4_2$
$a = b$, c (Å)	34.61(4), 16.510(17)
V (Å^3)	19777(45)
Z	4
D_{calc} (g/cm^3)	1.135
F (000)	6976.0
Resolution (Å)	7.0 – 0.85
No. of reflections for refinement	17466
Refined parameters	2450
R_1, wR_2 for $F_o > 4\sigma$ (F_o) (all data)	0.1647, 0.3722
Goodness of fit	1.929

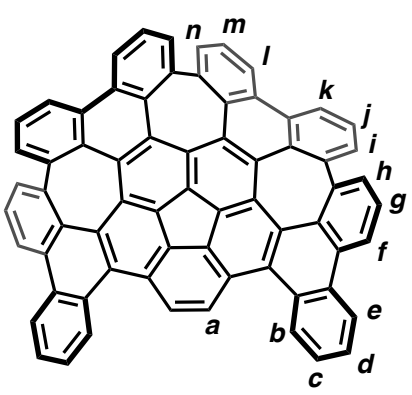

a	8.99
b	9.88
c	8.12
d	8.03
e	9.06
f	9.01
g	7.90
h	7.70
i	7.39
j	7.82
k	8.86
l	8.89
m	7.91
n	7.68

Fig. S5. The ^{1}H NMR chemical shifts (ppm) calculated by GIAO B3LYP/6-311+G(2d,p)//B3LYP/6-31G(d) level of theory. Tetramethylsilane (0.00 ppm) was used as a reference.

Table S2. Cartesian coordinates of the optimized structure of **1-H**.

C	3.975642	4.645339	-0.917983	C	-4.489203	1.359222	0.592980	C	1.229944	0.415077	-0.671898
C	4.945087	5.534158	-1.339230	C	-5.035331	2.385735	1.423360	C	0.010487	-0.283101	-0.729897
C	6.246586	5.079140	-1.596876	C	-4.550286	3.750186	1.265391	C	-1.057036	0.661913	-0.732384
C	6.532172	3.735291	-1.460579	C	-3.387234	3.973500	0.488647	C	-0.476943	1.941309	-0.639891
C	7.106142	0.863014	-1.317484	C	-1.795999	-3.360999	-1.058729	H	2.972495	5.018287	-0.781843
C	7.434506	-0.456551	-1.088343	C	-2.901842	-3.574221	-1.924494	H	4.690860	6.581254	-1.479255
C	6.570862	-1.249151	-0.324147	C	-4.021925	-2.645924	-1.856520	H	7.021789	5.771607	-1.913104
C	5.334303	-0.767301	0.098865	C	-3.932543	-1.518569	-0.990363	H	7.541874	3.399410	-1.664226
C	4.667382	-1.538465	1.180042	C	3.335169	-2.032030	1.149183	H	7.811107	1.494617	-1.844169
C	5.495614	-1.847994	2.262977	C	2.984610	-3.035114	2.097664	H	8.378016	-0.859890	-1.445050
C	5.061109	-2.670230	3.302967	C	1.812357	-3.863182	1.849221	H	6.872267	-2.249082	-0.027739
C	3.832114	-3.288244	3.195327	C	0.950242	-3.538477	0.766749	H	6.491692	-1.419187	2.294096
C	1.598600	-5.044434	2.588353	C	4.249983	3.267396	-0.714936	H	5.699765	-2.854105	4.162226
C	0.589820	-5.923325	2.250481	C	5.554728	2.803230	-1.039023	H	3.519971	-3.975127	3.972350
C	-0.193889	-5.660482	1.127556	C	5.861653	1.390175	-0.902952	H	2.255566	-5.297588	3.410740
C	-0.022273	-4.498535	0.369559	C	4.895870	0.519423	-0.321892	H	0.430370	-6.828156	2.830235
C	-0.880996	-4.424793	-0.842855	C	-0.241869	4.086280	0.289554	H	-0.963105	-6.365792	0.830937
C	-0.937490	-5.549930	-1.663314	C	-2.569511	2.842534	0.072781	H	-0.214310	-6.346130	-1.515033
C	-1.918175	-5.672554	-2.654388	C	-2.620153	-1.084430	-0.529244	H	-1.925937	-6.539228	-3.309380
C	-2.916252	-4.721114	-2.746436	C	-3.161031	1.535204	0.003500	H	-3.717444	-4.868238	-3.461323
C	-5.226799	-2.893780	-2.545585	C	1.063748	-2.223708	0.136782	H	-5.300763	-3.735022	-3.224453
C	-6.336564	-2.096529	-2.345319	C	-1.556667	-2.026692	-0.530824	H	-7.255632	-2.287185	-2.892317
C	-6.288476	-1.079631	-1.387867	C	2.302656	-1.484915	0.268406	H	-7.179308	-0.497566	-1.174575
C	-5.114695	-0.795970	-0.686745	C	3.506304	0.933197	-0.196249	H	-6.856638	-1.019418	1.217040
C	-5.251807	0.165662	0.442541	C	3.205300	2.323198	-0.330023	H	-7.509892	0.614383	2.971841
C	-6.320068	-0.080496	1.308909	C	1.144892	3.960553	0.230646	H	-6.450031	2.842890	2.992032
C	-6.707663	0.848230	2.277732	C	2.420052	-0.098973	-0.202651	H	-6.168978	4.714948	2.335104
C	-6.103151	2.089642	2.293693	C	-0.143189	-1.599494	-0.384746	H	-5.462876	6.999016	1.820946
C	-5.266949	4.865683	1.752734	C	-2.358838	0.371037	-0.406143	H	-3.513539	7.388978	0.305955
C	-4.883502	6.159757	1.446064	C	-1.142236	3.049550	-0.157582	H	-2.234303	5.473812	-0.554516
C	-3.782479	6.379590	0.604810	C	1.802917	2.777698	-0.265000	H	-0.632391	4.967568	0.784360
C	-3.053277	5.301813	0.134023	C	0.921416	1.802570	-0.657741	H	1.723809	4.753121	0.692151

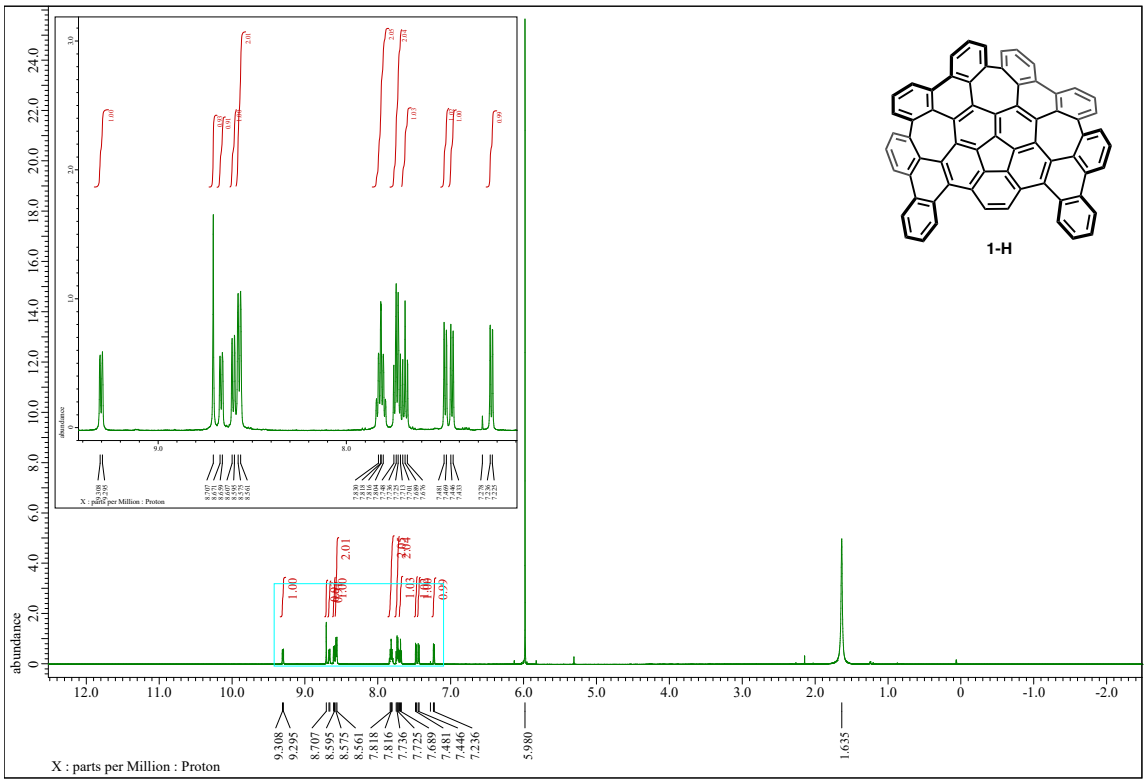

Fig. S6. ^{1}H NMR spectrum of **1-H** (600 MHz, $C_2D_2Cl_4$)

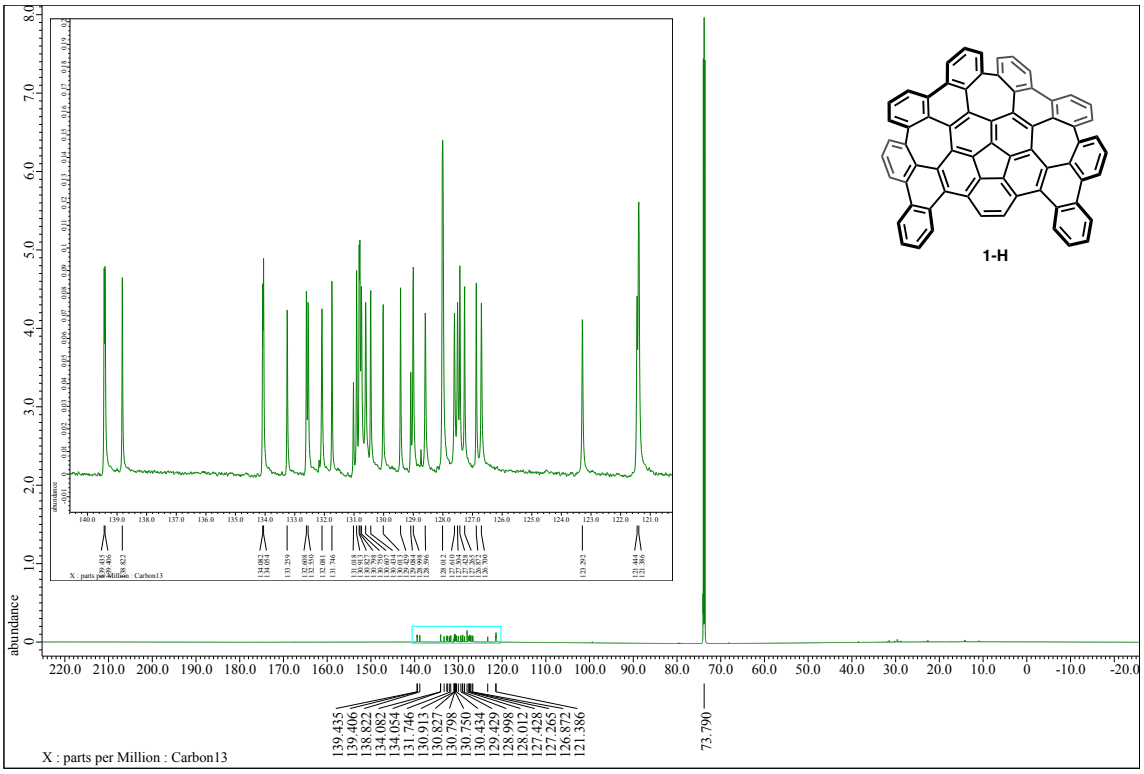

Fig. S7. ^{13}C NMR spectrum of **1-H** (150 MHz, $C_2D_2Cl_4$)

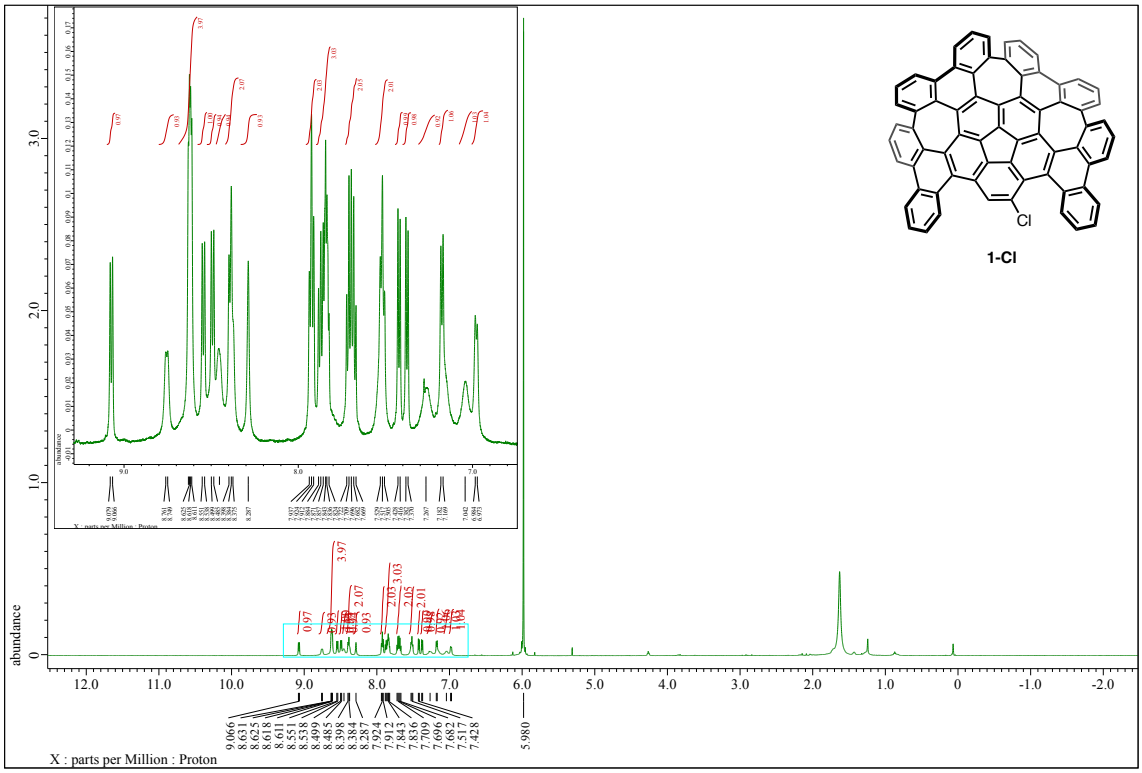

Fig. S8. ^{1}H NMR spectrum of **1-Cl** (600 MHz, $C_2D_2Cl_4$)

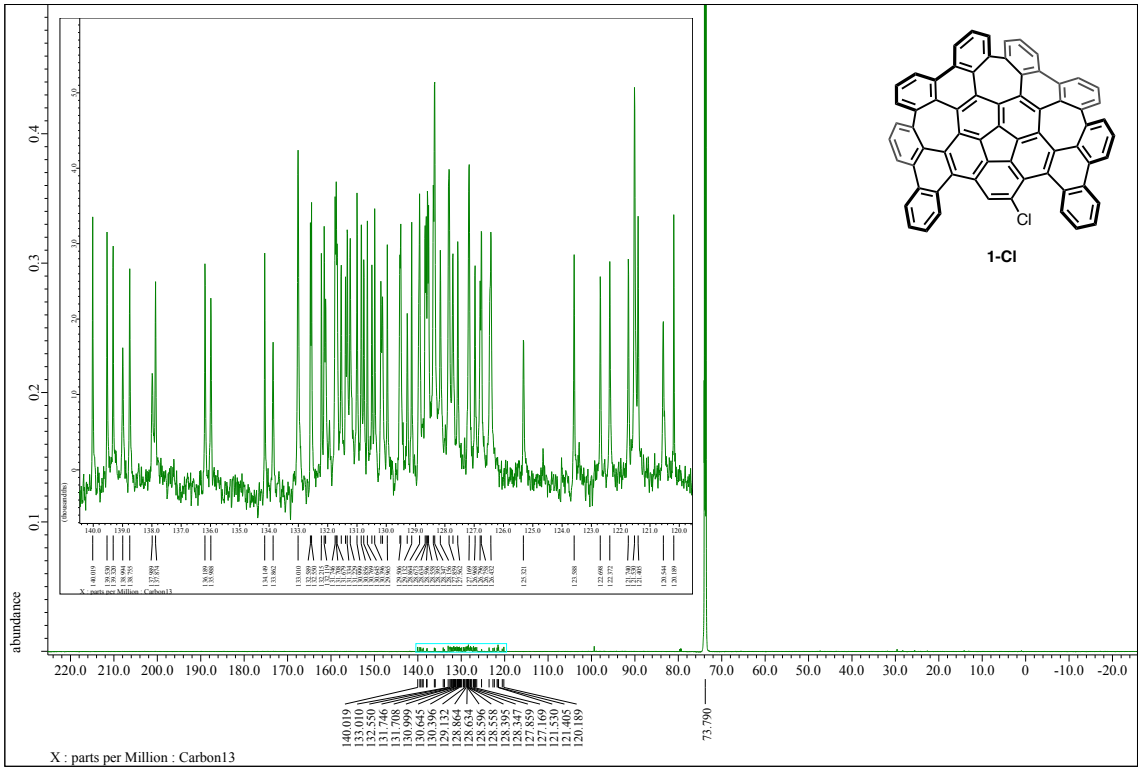

Fig. S9. ^{13}C NMR spectrum of **1-Cl** (150 MHz, $C_2D_2Cl_4$)

References

S1 Eliseeva, M. N.; Scott, L. T. Pushing the Ir-Catalyzed C-H Polyborylation of Aromatic Compounds to Maximum Capacity by Exploiting Reversibility. *J. Am. Chem. Soc.* **2012**, *134*, 15169–15172.

S2 Sheldrick, G. M. SHELXT - Integrated Space-Group and Crystal-Structure Determination. *Acta Crystallogr. Sect. A* **2015**, *71*, 3–8.

S3 Sheldrick, G. M. Crystal structure refinement with SHELXL. *Acta Crystallogr.* **C71**, 3–8 (2015).

S4 Dolomanov, O. V.; Bourhis, L. J.; Gildea, R. J.; Howard, J. A. K.; Puschmann, H. OLEX2: A Complete Structure Solution, Refinement and Analysis Program. *J. Appl. Crystallogr.* **2009**, *42*, 339–341.

S5 Mastronarde, D. N. Automated Electron Microscope Tomography Using Robust Prediction of Specimen Movements. *J. Struct. Biol.* **2005**, *152*, 36–51.

S6 Yonekura, K.; Ishikawa, T.; Maki-Yonekura, S. A New Cryo-EM System for Electron 3D Crystallography by EEFD. *J. Struct. Biol.* **2019**, *206*, 243–253.

S7 Hamaguchi, T.; Maki-Yonekura, S.; Naitow, H.; Matsuura, Y.; Ishikawa, T.; Yonekura, K. A New Cryo-EM System for Single Particle Analysis. *J. Struct. Biol.* **2019**, *207*, 40–48.

S8 Takaba, K.; Maki-Yonekura, S.; Yonekura, K. Collecting Large Datasets of Rotational Electron Diffraction with ParallEM and SerialEM. *J. Struct. Biol.* **2020**, *211*, 107549.

S9 Yamashita, K.; Hirata, K.; Yamamoto, M. KAMO: Towards Automated Data Processing for Microcrystals. *Acta Crystallogr. Sect. D Struct. Biol.* **2018**, *74*, 441–449.

S10 Kabsch, W. XDS. *Acta Crystallogr. Sect. D* **2010**, *66*, 125–132.

S11 Evans, P. R. An Introduction to Data Reduction: Space-Group Determination, Scaling and Intensity Statistics. *Acta Crystallogr. Sect. D Biol. Crystallogr.* **2011**, *67*, 282–292.

S12 Kabsch, W. Integration, Scaling, Space-Group Assignment and Post-Refinement. *Acta Crystallogr. Sect. D Biol. Crystallogr.* **2010**, *66*, 133–144.

S13 Foadi, J.; Aller, P.; Alguel, Y.; Cameron, A.; Axford, D.; Owen, R. L.; Armour, W.; Waterman, D. G.; Iwata, S.; Evans, G. Clustering Procedures for the Optimal Selection of Data Sets from Multiple Crystals in Macromolecular Crystallography. *Acta Crystallogr. Sect. D Biol. Crystallogr.* **2013**, *69*, 1617–1632.

S14 Karplus, P. A.; Diederichs, K. Linking Crystallographic Model and Data Quality. *Science* **2012**, *336*, 1030–1033.

S15 McCoy, A. J.; Grosse-Kunstleve, R. W.; Adams, P. D.; Winn, M. D.; Storoni, L. C.; Read, R. J. Phaser Crystallographic Software. *J. Appl. Crystallogr.* **2007**, *40*, 658–674.

S16 Sheldrick, G. M. Experimental Phasing with SHELXC/D/E: Combining Chain Tracing with Density Modification. *Acta Crystallogr. Sect. D Biol. Crystallogr.* **2010**, *66*, 479–485.

S17 Afonine, P. V.; Grosse-Kunstleve, R. W.; Echols, N.; Headd, J. J.; Moriarty, N. W.; Mustyakimov, M.; Terwilliger, T. C.; Urzhumtsev, A.; Zwart, P. H.; Adams, P. D. Towards Automated Crystallographic Structure Refinement with Phenix.Refine. *Acta Crystallogr. Sect. D Biol. Crystallogr.* **2012**, *68*, 352–367.

S18 Larson, A. C. in *Crystallographic Computing*, F. R. Ahmed Eds, (Munksgaard, 1970) pp. 291–294.

S19 Frisch, M. J. *et al. Gaussian 16, Revision B.01*, Gaussian, Inc., Wallingford CT, 2016.

S20 Becke, A. D. Density-Functional Thermochemistry. III. The Role of Exact Exchange. *J. Chem. Phys.* **1993**, *98*, 5648–5652.

S21 Lee, C.; Yang, W.; Parr, R. G. Development of the Colle-Salvetti Correlation-Energy Formula into a Functional of the Electron Density. *Phys. Rev. B* **1988**, *37*, 785–789.

S22 Szumigala, R. H.; Devine, P. N.; Gauthier, D. R.; Volante, R. P. Facile Synthesis of 2-Bromo-3-Fluorobenzonitrile: An Application and Study of the Halodeboronation of Aryl Boronic Acids. *J. Org. Chem.* **2004**, *69*, 566–569.